Open channel block by gadolinium ion of the stretch-inactivated ion channel in *mdx* myotubes

Alfredo Franco, Jr., Bruce D. Winegar, and Jeffry B. Lansman
Department of Pharmacology, School of Medicine, University of California, San Francisco, California 94143-0450 USA

ABSTRACT Currents flowing through single stretch-inactivated ion channels were recorded from cell-attached patches on myotubes from *mdx* mice. Adding micromolar concentrations of gadolinium to patch electrodes containing normal saline produced rapid transitions in the single-channel current between the fully open and closed states. The kinetics of the current fluctuations followed the predictions of a simple model of open channel block in which the transitions in the current arise from the entry and exit of Gd from the channel pore: histograms of the open and closed times were well fit with single exponentials, the blocking rate depended linearly on the concentration of gadolinium in the patch electrode, and the unblocking rate was independent of the concentration of gadolinium. Hyperpolarizing the patch increased the rate of unblocking (~*e*-fold per 85 mV), suggesting the charged blocking particle can exit the channel into the cell under the influence of the applied membrane field. The rate of blocking was rapid and was independent of the patch potential, consistent with the rate of ion entry into the pore being determined by its rate of diffusion in solution. When channel open probability was reduced by applying suction to the electrode, the blocking kinetics were independent of the extent of inactivation, suggesting that mechanosensitive gating does not modify the structure of the channel pore.

INTRODUCTION

Skeletal muscle myotubes from *mdx* mice, an animal model for human Duchenne muscular dystrophy (Bulfield et al., 1984) possess a novel type of mechano-transducing ion channel that is open for seconds at resting membrane potentials and closes when the membrane is stretched by applying suction to the patch electrode (Franco and Lansman, 1990*a*). Like stretch-activated channels in both normal muscle (Guharay and Sachs, 1984; Lansman and Franco, 1990*b*) as well as *mdx* muscle cells (Franco and Lansman, 1990*a*), stretch-inactivated channels are permeable to both monovalent and divalent cations. The single-channel conductance, however, is smaller when divalent cations carry charge, suggesting that divalent cations bind more strongly than do monovalent cations to a site within the channel during ion transport.

Lanthanide cations have been useful as transition state analogues for studying the Ca^{2+} binding sites of ion channels (cf. Lansman, 1990). Lanthanides have ionic radii close to that of Ca^{2+} and, like Ca^{2+}, they form primarily ionic complexes with oxygen donor groups (Nieboer, 1975). The lanthanide cation gadolinium (Gd) has an ionic radius of 0.105 nm, close to Ca^{2+}, which has an ionic radius of 0.106 nm at a coordination number of eight (Shannon, 1976). Gd, moreover, inhibits single-channel currents through stretch-activated channels with an affinity in the micromolar range (Yang and Sachs, 1989; Franco and Lansman, 1990*b*).

In this paper, we describe the results of experiments that investigated the blocking actions of Gd on currents through single stretch-inactivated ion channels in *mdx* myotubes, taking advantage of the exceptionally long open time of the stretch-inactivated channel to resolve discrete blocking and unblocking events. We show that the blocking kinetics are well described with a simple two-state model of open channel block. We also show that the blocking kinetics are independent of the extent of channel inactivation produced by the mechanosensitive gating mechanism, suggesting that the reduction in channel open probability produced by deforming the membrane does not alter the structure of the pore as probed by the blocking ion.

METHODS

The methods for preparing primary cultures of *mdx* myotubes have been described previously (Franco and Lansman, 1990*a*). Recordings of single-channel activity were made from cell-attached patches following the method of Hamill et al. (1981). Patch electrodes were made from Boralex hematocrit glass (Rochester Scientific, Rochester, NY) and had resistances of ~2 MΩ with standard saline in the electrode and isotonic potassium aspartate in the bath. The junction potential between the electrode filling solution and the bathing solution was zeroed before forming a seal and rechecked at the end of each experiment. Current signals were recorded with a List EPC-7 amplifier with a 50 GΩ feedback resistor. Currents were filtered with

Address correspondence to Dr J. B. Lansman, Department of Pharmacology, School of Medicine, University of California, San Francisco, CA 94143-0450.

0006-3495/91/06/1164/07 $2.00

an eight-pole, low-pass Bessel filter at 2 kHz (−3 dB) and sampled at 10 kHz. Recordings were made at room temperature (20–24°C).

Solutions

The patch electrode filling solution was a standard saline solution containing 150 mM NaCl, 5 mM KCl, 2 mM $CaCl_2$, 1 mM $MgCl_2$, 10 mM glucose, and 5 mM Hepes. The pH was adjusted to 7.5 with NaOH. Gadolinium (>99.9% purity; Aldrich Chemical Co., Milwaukee, WI) was added to the electrode filling solution directly as the chloride salt. Hydrolysis of gadolinium occurs at pH 7.5 (Smith and Martell, 1976), but because of the uncertainties in the determination of lanthanide affinity constants, the concentration of free trivalent was not calculated (see Lansman, 1990 for discussion).

The bathing solution (K-Asp) contained 150 mM aspartic acid, 150 mM KOH, 5 mM $MgCl_2$, 60 mM glucose, 1 mM EGTA, and 10 mM Hepes. The pH was adjusted to 7.4 by adding KOH. The isotonic K^+ bathing solution was used to zero the cell membrane potential so that the patch potential would be equal to the voltage command applied to the patch clamp amplifier. Comparing the single-channel current-voltage relation measured before and after excising the patch from the cell surface indicated a maximum voltage error of ~10 mV.

Measurement of the duration of open and blocked times

Open times were corrected for missed blockages when >20% of the events were missed. Because individual openings separated by a missed blocked period would be detected as a single event, the exponential fit to the open time histogram gives a mean open time that is larger than the true mean open time. The ratio of the number of missed blockages to the total number of blockages is given by

$$1 - \exp(-D/\mu_C) \quad (1)$$

where D is the dead time of the recording system and μ_C is the mean closed time obtained from the time constant of the exponential fit to the lifetime histogram (Colquhoun and Sigworth, 1983; Blatz and Magleby, 1986). Mean open times were corrected by multiplying the uncorrected mean open time by the ratio of the detected to the total number of blocking events and then subtracting the sum of the duration of all missed closings.

Analysis of the distribution of current amplitudes

At negative membrane potentials, the rate of unblocking became very fast. To obtain the rate constants for blocking and unblocking we analyzed the distribution of current amplitudes by fitting it to a beta function (FitzHugh, 1983; Yellen, 1984). The amplitude distribution, which included the blocking and unblocking events within a burst, was measured and compared to the theoretical beta function derived for a two-state process which is obtained by specifying the transition rates and the filter cut-off frequency. The numerically generated beta function was convolved with a Gaussian function fit to the closed channel noise and the transition rates changed to obtain the best fit by eye (see Winegar and Lansman, 1990). Current records were refiltered with a low cut-off frequency (100–200 Hz) so that blocking kinetics would be in a range, relative to the system bandwidth, where the single-pole filter approximation used to derive the beta distribution would be valid (see Yellen, 1984).

Power spectra of current fluctuations

The power density spectra of the current fluctuations produced by Gd blocking and unblocking were measured from records filtered at 2 kHz. The power spectrum of the closed channel noise in each experiment was subtracted from the power spectrum of the current fluctuations produced by Gd. The subtracted spectra were fit with a single Lorentzian function. For a simple transition between an open and blocked channel the Lorentzian should have a single time constant

$$\tau = 2\pi f_c^{-1} \quad (2)$$

where f_c is the corner frequency. For a two-state blocking reaction, the reciprocal of the time constant is the sum of the blocking and unblocking rates where

$$2\pi f_c = k_{off} + k_{on}[B] \quad (3)$$

and k_{off} is the unblocking rate and $k_{on}[B]$ is the product of the blocking rate and the blocking ion concentration. No correction was made for the filtered variance in the net power spectra (Ogden and Colquhoun, 1985).

RESULTS

Concentration dependence

Fig. 1 shows the effects of adding increasing concentrations of Gd to the patch electrode which contained physiological saline. The records are from different recordings from cell-attached patches in which the electrode contained the indicated concentration of Gd. As the concentration of Gd in the electrode was increased, the number of rapid transitions between the

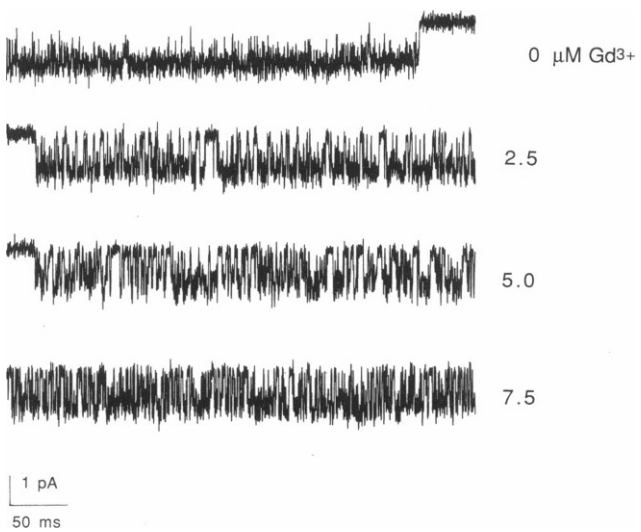

FIGURE 1 The unitary current in the presence of different concentrations of Gd in the electrode. Each record of channel activity is from a different patch with the indicated concentration of Gd in the electrode. Holding potential was −60 mV. Currents were filtered at 2 kHz.

open and closed channel levels increased. This behavior is consistent with a simple two-state model of open channel block in which Gd rapidly enters and exits the channel pore, blocking the flow of permeant ions during the time it resides within the channel (cf. Neher and Steinbach, 1978).

The two-state model predicts that the distribution of open and closed times within a burst of openings are exponentially distributed. In addition, the rate of blocking should increase with the concentration of blocker, while the rate of unblocking should be independent of the concentration of the blocker. These predictions were tested in Fig. 2. Fig. 2 *A* shows the open and closed time histograms from two experiments in which the electrode contained either 2.5 (*top*) or 7.5 μM (*bottom*) Gd. In both experiments, the histograms of open and closed times were well fit with a single exponential. The mean open time and closed times were obtained from the maximum likelihood fit to a single exponential and are indicated in the figure. The mean open time decreased from 1.9 ms in the presence of 2.5 μM Gd to 0.8 ms in the presence of 7.5 μM Gd. On the other hand, the mean closed time was ~0.6 ms in the presence of either concentration of Gd.

Fig. 2 shows the concentration dependence of the blocking kinetics from a number of experiments. Fig. 2 *B* shows the inverse of the mean open time (blocking rate) plotted as a function of the concentration of Gd in the electrode. As predicted by the two-state blocking model, the blocking rate depended linearly on the concentration of Gd. The slope of the relation between the blocking rate and the concentration of Gd gave a second-order rate coefficient of $\sim 2.3 \times 10^8\ M^{-1}s^{-1}$. As shown in Fig. 2 *C*, the unblocking rate was independent of the concentration of Gd in the electrode. The results support the interpretation that Gd produces the rapid transitions between the open and closed channel levels by rapidly entering and exiting the channel.

Voltage dependence

To determine whether the blocking site is within the channel (Woodhull, 1973), we investigated the effects of the patch potential on the kinetics of the current

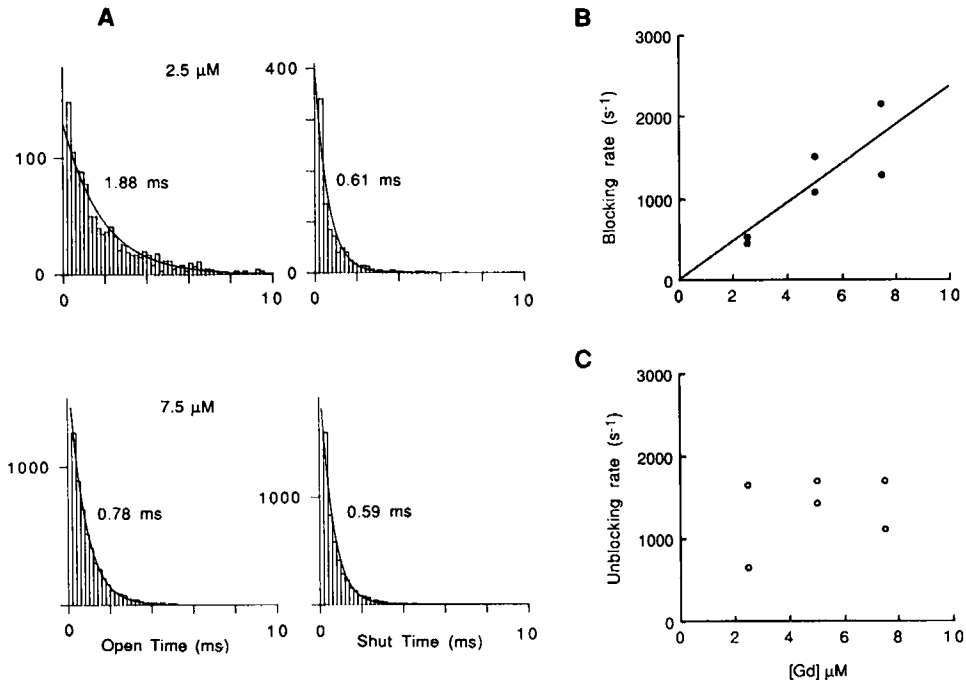

FIGURE 2 Analysis of the concentration dependence of the blocking kinetics. (*A*) Histograms of the durations of the open and closed times within a burst obtained from records like those shown in Fig. 1. Smooth curve through the histogram is the maximum likelihood fit with a single exponential. With 2.5 μM Gd (*top*), the mean open time was 1.88 ms and the mean closed time was 0.61 ms; with 7.5 μM Gd (*bottom*), the mean open time was 0.78 ms and the mean closed time was 0.59 ms. (*B*) The dependence of the blocking rate (1/mean open time) on the concentration of Gd in the electrode. The line through the experimental points is the least-squares linear regression line ($r = 0.86$) constrained to pass through the origin. The slope of the line gives a second-order rate coefficient of $2.3 \times 10^8\ M^{-1}s^{-1}$. (*C*) The dependence of the unblocking rate (1/mean closed time) on the concentration of Gd in the electrode.

fluctuations produced by a fixed concentration of Gd. Fig. 3 *A* shows records obtained in the presence of 5.0 μM Gd at −40, −80, −120, and −160 mV. At −40 and −80 mV, discrete transitions between the open and blocked states can be seen. At the more extreme hyperpolarized potentials, the blockages became quite brief.

At negative membrane potentials where the duration of the individual blocked times became too brief to detect as discrete events, we fit the distribution of current amplitudes with a beta function (see Methods). We measured the amplitude of the current in the presence of Gd during extended openings. Fig. 4 *A* shows the amplitude distribution of the current in the presence of Gd at −60 (*top*) and −120 mV (*bottom*) in the same patch. In these figures, the amplitude distribution represents the filtered blocking and unblocking of the open channel. The fit to a theoretical beta function is shown by the solid lines. At −60 mV, the fit to a beta function gave a blocking rate of 2,250 s^{-1} and an unblocking rate of 1,400 s^{-1}. In four experiments with 5 μM Gd in the electrode, amplitude distribution analysis gave a mean blocking rate of 2,425 ± 132 s^{-1} and a mean unblocking rate of 1,350 ± 526 s^{-1} (±SD). At −120 mV (Fig. 4 *A*, *bottom*), the unblocking rate increased to 2,175 s^{-1}, while the blocking rate did not change significantly (2,400 s^{-1}). The analysis suggests that the blocking rate does not depend on membrane potential, whereas unblocking becomes faster as the patch potential is made more negative.

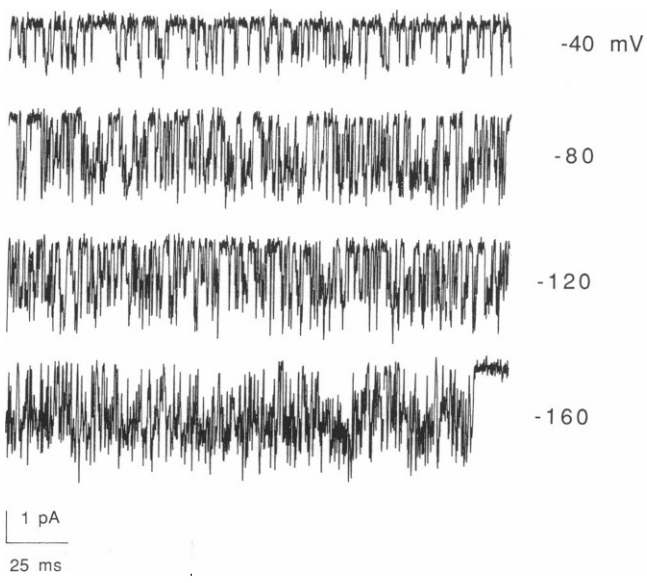

FIGURE 3 Voltage dependence of block in the presence of Gd. Records from a single recording from a cell-attached patch with 5.0 μM Gd in the electrode at the indicated patch potentials. The conductance in the presence of 5 μM Gd was 18 ± 4 pS (n = 3), compared with 23 ± 5 pS (n = 5) in the absence of Gd.

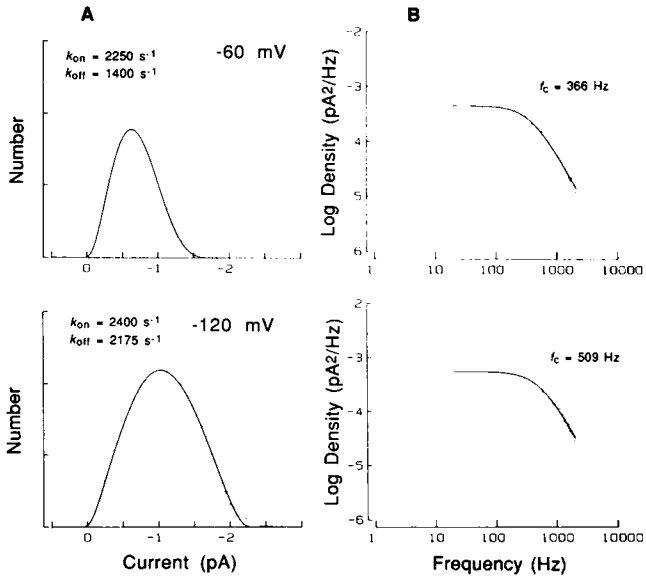

FIGURE 4 Analysis of the voltage-dependence of the block by Gd. (*A*) amplitude distributions of the current during a burst in the presence of 5 μM Gd at −60 (*top*) and −120 mV (*bottom*). The smooth curve through the experimental points is the fit to a numerically-generated beta distribution with blocking rates of 2,250 and 2,400 s^{-1} and unblocking rates of 1,400 and 2,175 s^{-1} at −60 and −120 mV, respectively. Current records were filtered at 100 or 200 Hz before measuring the distribution of current amplitudes. (*B*) Power density spectra of the current fluctuations in the presence of 5.0 μM Gd at −60 (*top*) and −120 mV (*bottom*). The smooth curve was drawn to a single Lorentzian of the form

$$S(f) = S(0)/1 + (f/f_c)^2$$

where the corner frequency f_c = 366 and 509 at −60 and −120 mV, respectively.

The two-state blocking model predicts that the power density spectra of the current fluctuations produced by the blocking ion should be fit by a single Lorentzian function in which the corner frequency is proportional to the sum of the blocking and unblocking rates. The power spectra were measured from the same experiment described above and these results are shown in Fig. 4 *B*. The power spectra were well fit with a single Lorentzian as expected for a simple two-state blocking process. In four experiments, the corner frequency for block produced by 5 μM Gd at −60 mV was 310 ± 45 Hz.

We compared the expected corner frequency predicted by the blocking and unblocking rates obtained from the amplitude distribution analysis with that measured directly by noise analysis check the correspondence between these two measurements. The fit of the amplitude distribution measured at −60 mV predicts a

corner frequency of ~580 Hz compared with that measured experimentally of 360 Hz. At −120 mV, the fit to a beta distribution predicts a corner frequency of 728 Hz, whereas the fit of a single Lorentzian to the power spectrum gave a time constant of 510 Hz. Although the rates obtained from the analysis of the amplitude distribution predict a corner frequency that is larger than that measured directly, the general agreement is good considering the methods used to analyze the blocking kinetics are different.

We also compared the blocking and unblocking rate constants obtained directly from the mean open and closed times within a burst over the voltage range of −40 to −80 mV where individual events could be resolved. Like the open and closed time histograms shown in Fig. 2*A* for records measured at −60, both were well fit with single exponentials suggesting the existence of a single open and blocked state over this voltage range. The inverse of the mean open time (blocking rate) and blocked time (unblocking rate) were plotted as a function of the patch potential in Fig. 5 (*filled squares*). The rate constants obtained from the fit of the amplitude distribution to a beta function over the entire voltage range (−40 to −160, open circles) are also plotted in Fig. 5. Fig. 5*A* shows that the blocking rate is independent of membrane potential over a wide range. Fig. 5*B*, on the other hand, shows that the unblocking rate increases with hyperpolarization (~*e*-fold per 85 mV). In both cases, there was good agreement between the measurement of the blocking rate constants by the fit of the amplitude distribution to a beta function and the direct measurement of the open and blocked times. The results indicate that the voltage dependence of channel block results solely from the voltage-dependent increase in the rate of unblocking.

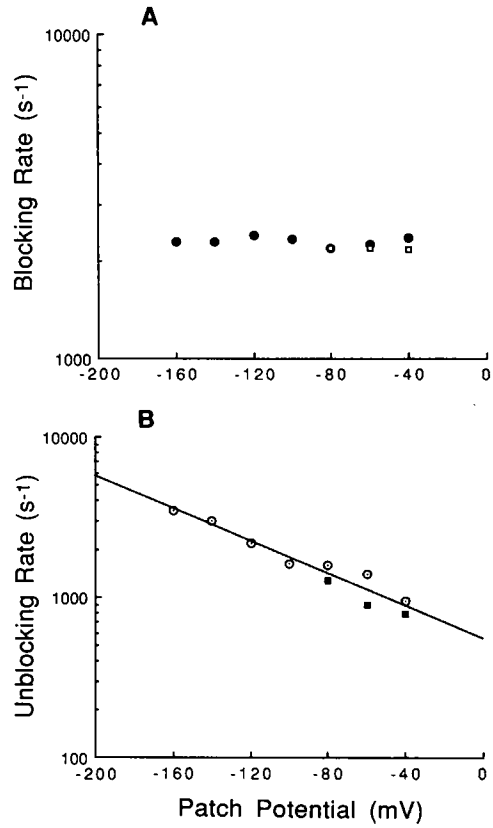

FIGURE 5 Dependence of the blocking and unblocking rates on membrane potential. (*A*) Dependence of the blocking rate on the patch potential. Open squares represent the inverse of the mean open time obtained from the single exponential fit to the histogram of open times. Filled circles are the rates obtained from the amplitude distribution analysis. (*B*) Dependence of the unblocking rate on the patch potential. Filled squares represent the inverse of the mean blocked time obtained from the exponential fit to the histogram of closed times. Open circles are the rates obtained from the amplitude distribution analysis. The line through the experimental points is the nonlinear least squares fit to a single exponential. The unblocking rate change *e*-fold/85 mV which corresponds to an effective electrical distance $\delta = 0.09$ for a trivalent blocking particle.

The blocking kinetics are independent of mechanosensitive gating

The open probability of the stretch-inactivated channel is reduced by applying suction to the patch electrode (Franco and Lansman, 1990*a*). To determine whether mechanosensitive gating alters the structure of the open channel, we examined the effects on the blocking kinetics of applying suction to the patch electrode. Fig. 6 shows the currents recorded in an experiment in which the patch electrode contained 5 μM Gd. In the absence of applied suction (0 mmHg), the rapid blocking and unblocking by Gd of the open channel appeared as long bursts of activity. Suction was subsequently applied to the electrode to inactivate the channel. Applying suction reduced in a graded and reversible manner the overall duration of the long channel bursts. This can be seen in Fig. 6 as a shortening of the apparent burst duration with the amount of suction applied to the electrode.

The relationship between the amount of suction applied to the electrode and the mean channel open probability in the presence of Gd is shown in Fig. 7*A*. In this experiment, each period during which suction was applied to the electrode was followed by a control period in which the suction was released. Channel open probability at each pressure was normalized to that measured during the subsequent return to zero applied pressure as a control for any slow rundown of channel activity. The normalized open probability decreased as the amount of suction applied to the electrode was increased as shown

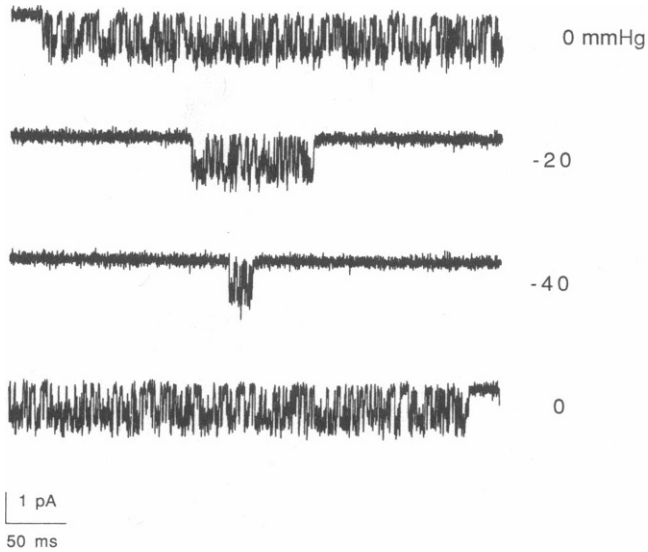

FIGURE 6 Effects of suction on single-channel currents measured in thet presence of Gd. Records are from an experiment in which suction was applied to the patch electrode which contained 5 μM Gd. The amount of suction applied is indicated next to the record. Holding potential was −60 mV. Current records were filtered at 2 kHz.

in Fig. 7*A*. The smooth line through the experimental points was drawn to a Boltzmann relation with half-inactivation = −17 mmHg and steepness = 6 mmHg. This compares with the stretch-inactivation curve measured in the absence of blocking ion in which half-inactivation = −11 mmHg and the steepness = 6.3 mmHg (Franco, A., Jr., and J.B. Lansman, manuscript submitted for publication). Apparently, steady-state stretch inactivation is not altered by the presence of the blocker.

The blocking and unblocking rates were measured for records like those shown in Fig. 6, in which different amounts of suction were applied to the electrode to produce different degrees of inactivation. Fig. 7 *B* shows the results of this experiment in which the blocking rate (*filled circles*) and unblocking rate (*open triangles*) are plotted as a function of the amount of suction applied to the electrode. As can be seen in Fig. 7*B*, the rate constants for blocking and unblocking did not depend on the extent of channel inactivation over a wide range of channel open probability.

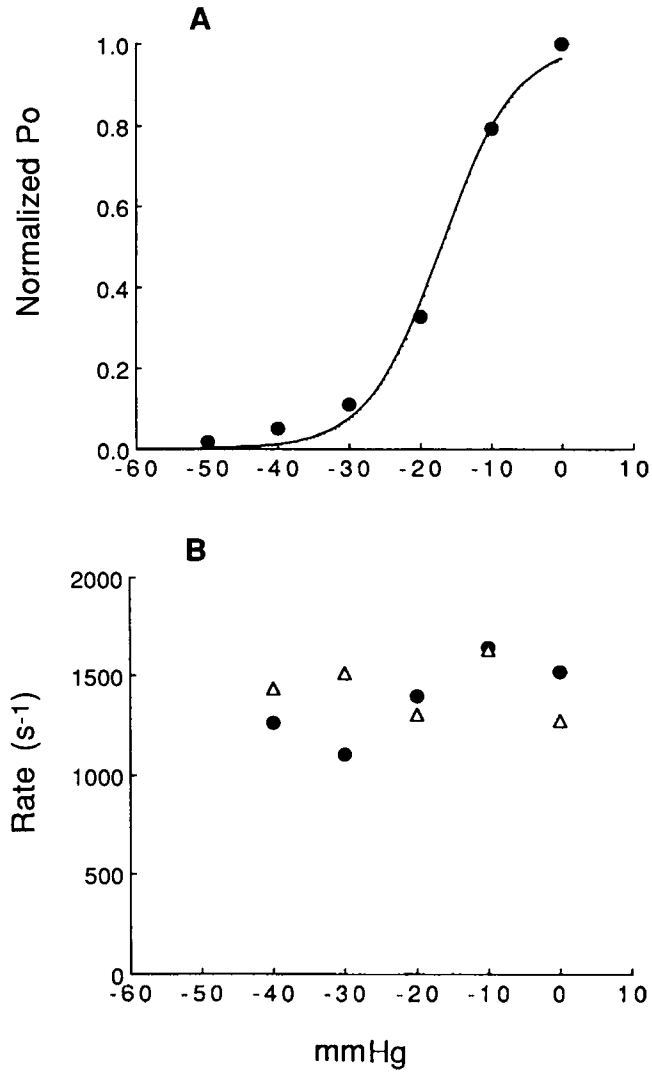

FIGURE 7 Dependence of the blocking kinetics on the extent of steady-state inactivation by stretch. (*A*) The dependence of channel open probability on the amount of suction applied to the electrode. The smooth curve was drawn to a Boltzmann relation with $P_{1/2}$ = −17 mmHg and Steepness 6.0 mmHg. (*B*) The blocking rate (*filled circles*) and the unblocking rate (*open triangles*) plotted as a function of the amount of suction applied to the electrode. Comparison with the curve in *A* shows that the rates of blocking and unblocking varied little over the entire inactivation range.

DISCUSSION

The use of a transition state analogue of Ca^{2+} allowed us to observe directly the blocking and unblocking of open mechanosensitive ion channels at the single-channel level. We find that Gd inhibits current through stretch-inactivated channels by entering and occluding the channel pore. The main new finding presented here is that the residence time of the blocking ion within the channel is not altered when the patch membrane is deformed by applying suction to the electrode. Apparently, mechanosensitive gating does not produce major modifications of the structure of the channel pore as probed by the blocking ion.

Mechanism of block

Channel block produced by Gd depends on membrane potential in such a way that hyperpolarization enhances the rate of unblocking. The effect of membrane potential on unblocking suggests that Gd can traverse the channel and exit to the cell under the influence of the applied membrane field. The block by Gd is similar to the block of single voltage-gated Ca^{2+} channels by Ca^{2+} and lanthanide cations (Lansman et al., 1986; Lansman, 1990). Block of the stretch-inactivated channel by Gd, however, is much less sensitive to membrane potential than block of voltage-gated Ca^{2+} channels ($\sim e$-fold/85 mV vs. $\sim e$-fold/25 mV, respectively). If it is assumed that Gd substitutes for Ca^{2+} at its channel binding site(s), then the difference in the sensitivity of the rate of unblocking to membrane potential suggests that the location of the Ca^{2+} complexation site within the channel also differs.

We find that the blocking rate is extremely rapid ($\sim 2.3 \times 10^8\ M^{-1}s^{-1}$) and near the limit of the rate of diffusion of the ion in free solution (Diebler et al., 1969). That the blocking rate was independent of membrane potential is consistent with a diffusion-limited process which would be expected to lie outside the membrane field. The absolute value of the blocking rate is similar to that reported by Yang and Sachs (1989) for the block of the stretch-activated channel in *Xenopus* oocytes ($1.6 \times 10^8\ M^{-1}s^{-1}$).

Our results show that Gd does not alter the relationship between channel open probability and pressure, consistent with the results of Yang and Sachs (1989) who found that the sensitivity of the stretch-activated channel to pressure in *Xenopus* oocytes was not greatly altered in the presence of Gd. On the other hand, the block of the stretch-inactivated channel described here differs from the block of stretch-activated channel (Yang and Sachs, 1989; Franco and Lansman, 1990*b*) in that Gd does not reduce the amplitude of the unitary current over a range of concentrations (Fig. 1). Information on the kinetics of blocking and unblocking of both stretch-activated and stretch-inactivated channels will be helpful for understanding the structural features of the permeation pathway of mechanosensitive channels.

Received for publication 13 November 1990 and in final form 17 January 1991.

REFERENCES

Blatz, A. L., and K. L. Magleby. 1988. Correcting single channel data for missed events. *Biophys. J.* 49:967–980.

Bulfield, G., W. G. Siller, P. A. Wight, and K. J. Moore. 1984. X chromosome-linked muscular dystrophy (*mdx*) in the mouse. *Proc. Natl. Acad. Sci. USA.* 81:1189–1192.

Colquhoun, D., and F. J. Sigworth. 1983. Fitting and statistical analysis of single channel records. In Single-channel recording, B. Sakmann and E. Neher, editors. Plenum Publishing Corp., New York. 191–263.

Diebler, H. M., M. Eigen, G. Illgenfritz, G. Maas, and R. Winkler. 1969. Kinetics and mechanism of reactions of main group metal ions with biological carriers. *Pure Appl. Chem.* 20:93–115.

FitzHugh, R. 1983. Statistical properties of the asymmetric random telegraph signal with applications to single-channel analysis. *Math. Biosci.* 64:75–89.

Franco, A., Jr., and J.B. Lansman. 1990*a*. Calcium entry through stretch-inactivated ion channels in *mdx* myotubes. *Nature* (Lond.). 344:670–673.

Franco, A., Jr., and J. B. Lansman. 1990*b*. Stretch-sensitive channels in developing muscle cells from a mouse cell line. *J. Physiol.* (Lond.). 427:361–380.

Guhary, F., and F. Sachs. 1984. Stretch activated single channel currents in tissue-cultured embryonic chick skeletal muscle. *J. Physiol. (Lond.).* 352:685–701.

Hamill, O. P., A. Marty, E. Neher, B. Sakmann, and F. J. Sigworth. 1981. Improved patch-clamp techniques for high resolution current recording from cells and cell-free membrane patches. *Pfluegers Arch. Eur. J. Physiol.* 391:85–100.

Lansman, J. B. 1990. Blockade of current through single calcium channels by trivalent lanthanide cations. Effect of ionic radius on the rates of ion entry and exit. *J. Gen. Physiol.* 95:679–696.

Lansman, J. B., P. Hess, and R. W. Tsien. 1986. Blockade of current through single calcium channels by Cd^{2+}, Mg^{2+}, and Ca^{2+}. Voltage and concentration dependence of calcium entry into the pore. *J. Gen. Physiol.* 88:321–347.

Neher, E., and J. H. Steinbach. 1978. Local anesthetics transiently block currents through single acetylcholine receptor channels. *J. Physiol. (Lond.).* 277:153–176.

Nieboer, E. 1975. The lanthanide ions as structural probes in biological and model systems. *Structure and Bonding.* 22:1–47.

Ogden, D. C., and D. Colquhoun. 1985. Ion channel block by acetylcholine, carbachol, and suberyldicholine at the frog neuromuscular junction. *Proc. R. Soc. Lond. B. Biol.* 225:329–355.

Shannon, R. D. 1976. Revised effective ionic radii and systematic studies of interatomic distances in halides and chalcogenides. *Acta Crystallogr.* A32:751–767.

Smith, R. M., and A. E. Martell. 1976. Critical Stability Constants Volume 4: Inorganic Complexes. Plenum Publishing Corp., New York & London. 2–3.

Winegar, B., and J. B. Lansman. 1990. Voltage-dependent block by zinc of single calcium channels in mouse myotubes. *J. Physiol. (Lond.).* 425:563–578.

Woodhull, A. 1973. Ionic blockage of sodium channels in nerve. *J. Gen. Physiol.* 61:687–708.

Yang, X., and F. Sachs. 1989. Block of stretch-activated ion channels in *Xenopus* oocytes gadolinium and calcium ions. *Science (Wash. DC).* 243:1068–1071.

Yellen, G. 1984. Ionic permeation and blockade in Ca^{2+}-activated K^+ channels of bovine chromaffin cells. *J. Gen. Physiol.* 84:157–186.